ORIENTAL JOURNAL OF CHEMISTRY
An International Open Access, Peer Reviewed Research Journal
www.orientjchem.org
ISSN: 0970-020 X
CODEN: OJCHEG
2025, Vol. 41, No.(1):
Pg. 264-273

Synthesis, Characterisation, Biological activities of Transition Metal Complexes Derived from Alloxan

PADMA PRIYA GOPALAKRISHNAN*[1,2] and GIRIJA CHAMARAHALLI RAMAKRISHNA IYER*[3]

[1]Research and Development Centre Bharathiyar University, Coimbatore, India.
[2]Deparment of Chemistry and Biochemistry Jain University Bengaluru, India.
[3]Department of Chemistry, SSMRV Degree College Bangalore, India.
*Correspondence author E-mail: g.padmapriya@jainuniversity.ac.in

http://dx.doi.org/10.13005/ojc/410131

(Received: October 14, 2024; Accepted: January 05, 2025)

ABSTRACT

Schiff-bases have acquired attention because of their flexible structural design and wide range of uses. In order to enhance the biological component of d block elements, our current study has been conducted to synthesize a variety of Schiff-base complexes. A weakly basic molecule results from the condensation of a keto or an aldehyde group [C=O] with an amine or amino compound. Designing novel therapeutic medications is made possible by medicinal inorganic chemists in a number of ways. This is due to the wide variety of coordination number and geometries, various redox states, thermodynamic properties, kinetic properties, and distinctive properties of the metal ions being available. Alloxan- 2,4,5,6[1H,3H] pyrimidinetetrone is a heterocyclic compound with high biological and physiological effect on living organisms A potential path toward the development of new materials with a wide range of applications is offered by organometallic complexes. A foundation for developing drugs that may be applied in a variety of settings is provided by the electrical changes that take place between metal-ligand complexes. Schiff base ligand and its metal acetyl acetonate complex is synthesised in an ecofriendly way using microwave assisted reaction.

Keywords: Alloxan orthophenylenediimine, Acetyl acetonate complexes, UV, IR, HNMR, TGA antibacterial, Docking.

INTRODUCTION

According to a review of the literature, substituted amine complexes with transition metals may not have received enough attention. The structure and activity characteristics of alloxan thiosemicarbazones and alloxan substituted thiosemicarbazone complexes were examined due to the pharmacological significance of Au(IH)[1-10].

The lack of references in the literature that address aromatic diamines and carbonyl type Schiff base metal complexes results in a gap in understanding properties of Schiff base metal complexes with quadridentate ligands. The creation of polydentate Schiff bases may result from the addition of many donor atoms and their

This is an Open Access article licensed under a Creative Commons license: Attribution 4.0 International (CC- BY).
Published by Oriental Scientific Publishing Company © 2018

combination. Oxygen-nitrogen (O-N), oxygen-nitrogen-sulfur (O-N-S), oxygen-sulfur (O-S), and nitrogen-sulfur (N-S) are a few important donor atoms[11-14]. The ligands produced from diamines and dicarbonyl compounds are useful chelating agents in addition to being crucial in biological processes. Open chain bi, tri, tetra, or multidentate ligands are the focus of the majority of current research.

The synthesized ligand Alloxan orthophenylenediimine and oxo vanadium, zirconium complexes are characterized using UV-Vis, Molar conductance, IR, NMR, TGA and screened for their antibacterial. The ligand and complexes are tested for their antimicrobial activities using well diffusion methods.

EXPERIMENTAL

Ligand Preparation

Alloxan orthophenylenediimine was prepared in an environmental sustainable method. The reaction is catalyzed using citric acid (lemon) in place of an acid (1.60 g 0.001 M) solution of parent compound in methanol was condensed with (1.08g 0.001M) solution of Orthophenylene diamine dissolved in ethanol. The reaction mixture is made homogenous using magnetic stirrer. The reaction is conducted using microwave radiation for 2 to 3 minutes. The reaction completion is identified using (TLC) plates. The reaction was permitted to progress until the original compound site was completely exhausted. The reaction mixture was kept for slow evaporation for 48 hours. The resulting precipitate was filtered using suction pump, was subsequently thoroughly cleaned with methanol to remove any coloured impurities.

Filtered yellow coloured precipitate was dried in a desiccator in vacuum. The reaction is conducted using microwave irradiation for a duration of approximately 4 to 5 minutes. The application of this technique led to a greater output of products, suggesting enhanced efficacy, in contrast to the yield obtained using conventional heating approaches in similar circumstances, which did not exceed 60%.

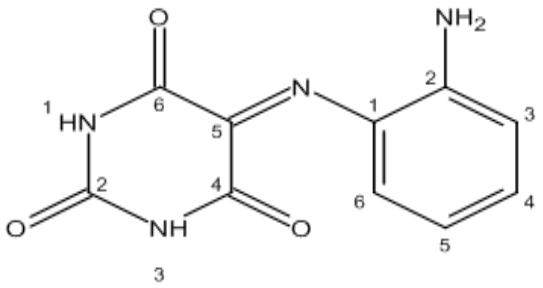

Fig. 1. 5-(2-aminophenyl)imino)pyrimidine-2,4,6(1H,3H,5H)-trione)

Synthesis of metal complexes of L_1-Vanadium oxy acetyl acetonate and Zirconium acetyl acetonate

Hot methanolic solution of L_1 (0.5 g 0.001M) and hot ethanolic solution of (0.53 g 0.001M)VO $(acac)_2$ were mixed in the ratio 2:1 and refluxed using condenser for 4 to 5 hours. The fundamental criterion for the formation of complexes was determined to be the manifestation of a distinct colour change arising from the amalgamation of ligand and metal. After being subjected to a three-day evaporation process, a green solid mono-nuclear metal complex was formed. The precipitation occurred subsequent to the process of cooling. The anhydrous complexes that were synthesised was filtered, followed by rinsing with methanol and subsequent drying under vacuum. The approach described in the experiment allowed for the observation of the quantitative yield.

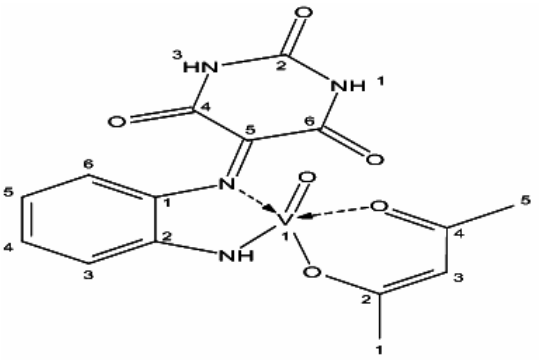

Fig. 2. Structure of L_1–VO (acac) complex

Hot methanolic solution of L_1 and ethanolic dissolved (0.48 g 0.001M) Zr $(acac)_4$ in the ratio 2:1 were mixed together and refluxed in condenser for approximately 5 h in presence of DMF which provides optimum pH condition. The identification of a shift in hue within the amalgamation of substances was regarded as the principal indication of the creation of the complex. Subsequently, the reaction mixture was subjected to a cooling procedure utilising an ice bath, leading to the formation of a solid metal complex. Following a three-day

evaporation process, the resulting luminous green complex was clarified, subsequently lapped with cold methanol, and finally using anhydrous calcium chloride it is vacuum dried.

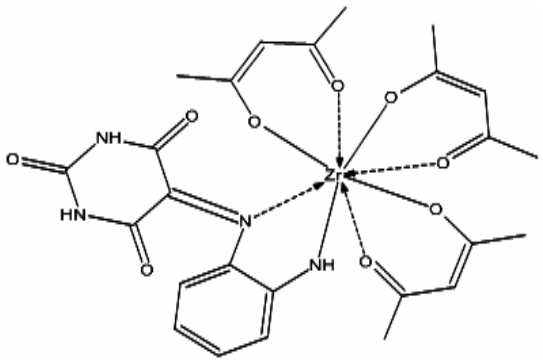

Fig. 3. Structure of L_1-Zr(acac)$_3$ complex

Study of Antimicrobial Property of the Synthesized Ligand and complexes

The *In-vitiro* antibacterial activity of the synthesized Schiff base ligand and its metal complexes were evaluated against bacterial strains including *Pseudomonas aeruginosa*, *Escherichia coli, Bacillus cereus*. The biological activity of the synthesized ligand were investigated for its antibacterial activity using Agar well diffusion method which is used as bacterial sensitivity test. The sample was assessed with three bacterial cultures. Two gram negative and one gram positive bacteria were considered to evaluate biological activity. The ligand and complexes activity were compared against a standard drug streptomycin which was used as a control.

Molecular docking studies of Thymidine phosphorylase with L_1 VO (acac) complex

Given that thymidine phosphorylase is frequently overexpressed in several types of cancer, blocking it with ligands may have therapeutic advantages, especially when it comes to specific illnesses and ailments. Vina docking was used to examine the activity of L_1 and their VO (acac) complexes in order to investigate the nature of inhibition. In this docking studies AD4 docking results for ligands L_1 with VO and with Zirconium were obtained by replacing with other metals to test their docking performance.

RESULTS AND DISCUSSION

Molar Conductivity and magnetic susceptibility L_1 and its complexes

The ligand and the complex synthesized were physico chemically characterized by elemental analysis and several analytical methods. Table 1 provides the C, H and N data for the ligand and its complexes. They agreed well with formal empirical calculations. A conductivity meter was used to measure the conductivity of the ligand and complexes. Complexes were completely soluble in DMSO, whereas slightly soluble in alcohols.

The empirical formula, nature of coordinating group with metal complex required to be studied to understand molar conductance data. Identifying electrolytic or non-electrolytic nature of metal complex is the first step in applying molar conductance data. The conductivity values of the ligand lies above the value 18.9 to 35.4 $\Omega^{-1}cm^2mol^{-1}$ suggesting electrolyte nature of the ligand and non-electrolytic nature of complex. Molar conductance value gives useful information about metal to ligand stoichiometries. Those complexes with 1:2 metal-ligand stoichiometry have lower molar conductance as compared with analogue complex with 1:1 stoichiometry. In Vanadium and Zirconium complex the ratio of metal to ligand lie between 1:2 and 1:4 which is indicated by lower molar conductance value. The magnetic moments obtained for the oxo-vanadium (IV)d^1 configuration lie in the range 1.76 to 1.82 Bohr magneton values are close to spin only values of the complexes hitherto reports suggest. The results preface the exchange interactions in these complexes. Zr(IV)d^0 configuration exhibit diamagnetic property which is evident from the observed diamagnetic values.

Table 1: Analytical Data for L1 and complexes

Compound	Colour	m. p. (°C)	Found (Calc)% C	H	N	ΛM*	μeff (BM)	Geometry
Alloxan -OPDI	Yellow	280	51.89 51.72 3.44	3.24 24.13	24.78	196.8	-	-
L_1-VO (acac)	Green	330 45.34	45.76 3.52	3.69 14.1	14.65	26.8	1.76	Square pyramidal
L_1-Zr (acac)$_3$	Fluorescent green	345	48.96 48.46	4.28 4.53	25.49 25.57	30	Diamagnetic	Square antiprismatic

Electronic (U-V Visible spectra) of L_1 and its complexes

The UV-Visible Labman-1200 spectrometer has been used to study the ligand and complex optical behaviour. The step scan has fixed at 1 ns, and the wavelength region has fixed between 190 and 800 nm. For these ligands, dimethyl sulfoxide has been used as the solvent. A concentration of 0.1 g/mL has been used for each ligand, and complexes and the UV-Visible spectrum has been created after the absorption and transmission spectra have been recorded. The electronic absorption spectroscopy tool is used for distinctive the characterization for ascertaining the binding mode of complexes. The maximum absorbance ranges in the region between 250 to 300 nm which is due to Alloxan forming C=N with OPD resulting in Schiff Base. This absorbance is attributed to both ligand and metals complexes of L_5 involving $\pi \rightarrow \pi^*$.

The electronic spectra of oxovanadium complexes (IV) exhibit three band in the region 22300-13200 cm^{-1}. Several models have been proposed for the interpretation of ES of oxovanadium complexes (Selbin.J 1966 *et al.,*) Among the various proposed models Ballhausen–Gray model received independent support from an entirely related ligand field approach. The model stands supportive for interpretation of results of VO^{2+} complexes. The isolated oxovanadium (IV) complexes show expected three bands and the anticipated spectra have identical types signifying geometry around vanadium atom. The three bands in the region constitute13200-13600 cm^{-1}, 16300-16750 cm^{-1}, 21500-23000 cm^{-1}. The first band appears as broad, second occurs as a weak band. The third band appearing at 2300 cm^{-1} is attributed to charge transfer between dz^2 of V and $2p_x$, $2p_y$ orbital of O_2 atom. The first and second bands are assigned to $^2B_2 \rightarrow {}^2E$ and $^2B_2 \rightarrow {}^2B_1$ (Selbin.J;1966) which suggest d-d transition. On the basis of the data available square pyramidal geometry has been assigned to L_1VO acac complexes.

Shoulder band at 375 nm is apportioned to the n-π^* transitions due to imine chromophore illustrates a bathochromic shift zirconium complexes. This band shifts considerably to the higher-energy in the $Zr(acac)_3$ complexes due to the polarization caused by the zirconium-ligand electron interaction. The spectra of Zr complex shows high intense absorption region at 28300-29200 cm^{-1} indicating a high coordination number. Due to Zr(IV)d^0 electronic configuration, there are no d-d transitions but two absorption band centered at 24550-24350 cm^{-1} which is distributed to charge transfer transition. Spectral data indicates a higher coordination number and they bear a resemblance to those complexes with square antiprismatic configuration.

FT-IR spectral studies

The coordination mode of L_1 in complexes is identified based on the tentative assignments of infrared (IR) of the synthesises L_1VO and Zr $(acac)_3$ complexes are given in Table 2. The IR spectra of ligand and metal complex is depicted in Fig. 4 reveals the Schiff base formation with a band appearing in the region1649-1664 cm^{-1}. A medium intensity band due to ascribed vibrations of $\upsilon_{(C=N)}$ at 1625–1650 cm^{-1} in the spectra it is shifted to lower wavenumber in L_1 complexes under study shows the coordination of azomethine nitrogen to the metal atom. The presence $\upsilon_{(N-H)}$ asymmetric stretching vibration, in alloxan shows triplet absorption bands appearing at ~3485, 3491, and 3496 cm^{-1} appeared in ligand and complexes. Ligands and complexes exhibited medium to high intensity bands ~1370, 1377, 1390 cm^{-1} due to symmetric stretching vibration of $\upsilon_{(NH)}$. This $\upsilon_{(NH)}$. bending has shifted from 1390 cm^{-1} upon complexation designating contribution of NH_2 complex formation. High intensity band appearing in the region1725-1740 cm^{-1} is attributed to $\upsilon_{(C=O)}$ of Alloxan.The band at 1390 is lowered to 1377, 1370 cm^{-1} suggesting coordination through nitrogen of diphenyl amine of OPD. The out-of-plane $\upsilon_{(C-H)}$ deformation of the phenyl ring was observed at 750 cm^{-1}. The IR spectra of vanadyl complexes display a strong band in the region 1000-950 cm^{-1} due to V=O group which is absent in ligand. The IR spectra of the oxovanadium complexes containing strong peak at around 990 cm^{-1} which is assigned to stretching mode of non-bridging V=O group. The bands at 2156 cm^{-1}, 2175 cm^{-1} indicates presence of $\upsilon_{(C=C=O)}$ due to metal acac whereas in ligand it is absent. The band at 638 $cm^{-1}$and 630 cm^{-1} suggest presence of metal $\upsilon_{(M-L)}$ coordination with the ligand. The coordination of imine to the metal atom is reinforced by the presence of a new absorption band at 535 cm^{-1}, is due to (Zr $\leftarrow$ N) vibrations . It is further inveterate showing sharp band at 1035-1040 cm^{-1} in the spectra of $L_1Zr(acac)_3$ isassignable to (Zr $\leftarrow$ O) stretching vibrations.

Table 2: Assignment FTIR Analysis of AOPDI : L_1 and its VO and Zr acac Complexes

	Wavenumber cm^{-1}									
L_1/complex	(N-H)	(C=O)	(C=N)	Aromatic CH ring	C-NH	Ar(C=C)	(C=C=O)	(C-H)	(M-N)	(M-O)
AOPDI	3496	1740	1664	3040	1390	*	*	1331		
AOPDI VO acac	3491	1739	1658	3047	1377	1500	2156	1320	990	638
AOPDI Zr acac	3485	1725	1649	3039	1370	1589	2145	1325	*	630

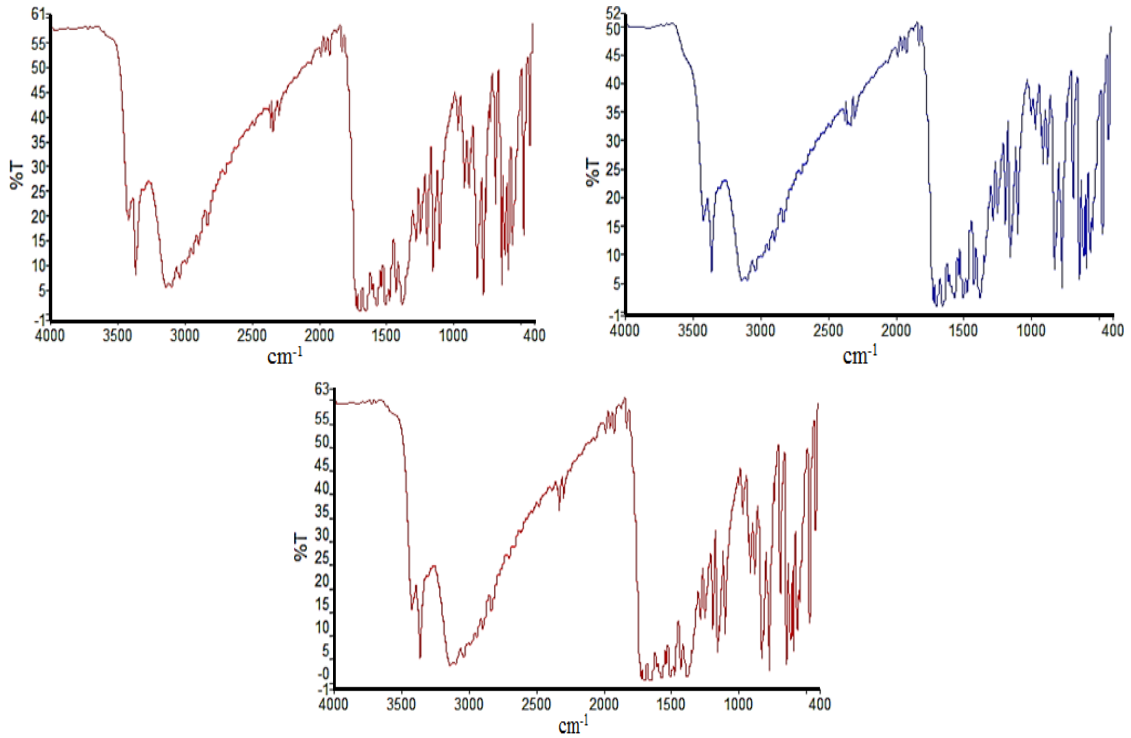

Fig. 4. FTIR Spectrum of AOPDI:Ligand and its VO and Zr acac complex

^{1}H NMR of L1 and its complexes

^{1}H NMR (DMSO-d6) spectrum of the L_1Voand Zr (acac) displayed in Table 3 the following resonance signals are observed corresponding to resonance absorption due to imino proton signal at δ11.09–13.01 ppm (s, H) (L_1)due to alloxan moiety. There is a multiplets centered at δ7.92 ppm due to (m A proton), δ7.65 ppm (m B proton) which correspond to aromatic ring hydrogen of orthophenylene diamine. Synthesised ligand shows a resonance signal at δ7.75corresponding to resonance absorption of the amide NH_2 group. However there is a small up field shift in oxovanadium and zirconium complexes due to complexation with metal ions. A multiplet centered signals in ligand are reduced to doublets (A and B protons) metal complexes of VO and Zr suggest that an H is lost during the coordination with the metal forming an imino proton –(NH). Interestingly peak at 3.3.ppm corresponds CH proton in metal acetyl acetonate which involves in keto-enol tautomerism. Signal at 2.2 ppm corresponds to CH_3 protons of acac. Spectra depicted in Figure 5.

Table 3: Assignment FTIR Analysis of AOPDI : L_1 and its VO and Zr acac complexes

		Wavenumber cm^{-1}				
Sr. No	Ligand Formula	Aromatic C-H proton	Alloxan ring N-H proton	NH_2 proton	CH proton acac	CH_3 proton acac
1	$C_{10}H_8N_4O_3$	7.92(A), 7.65(B)	11.09, 13.05	7.75	-	-
2	$C_{15}H_{14}N_4O_6V$	7.91(A), 7.65(B)	11.09, 13.01	7.71	3.3	2.2
3	$C_{25}H_{28}N_4O_9Zr$	7.86(A), 7.65(B)	11.08, 13.00	7.74	3.4	2.2

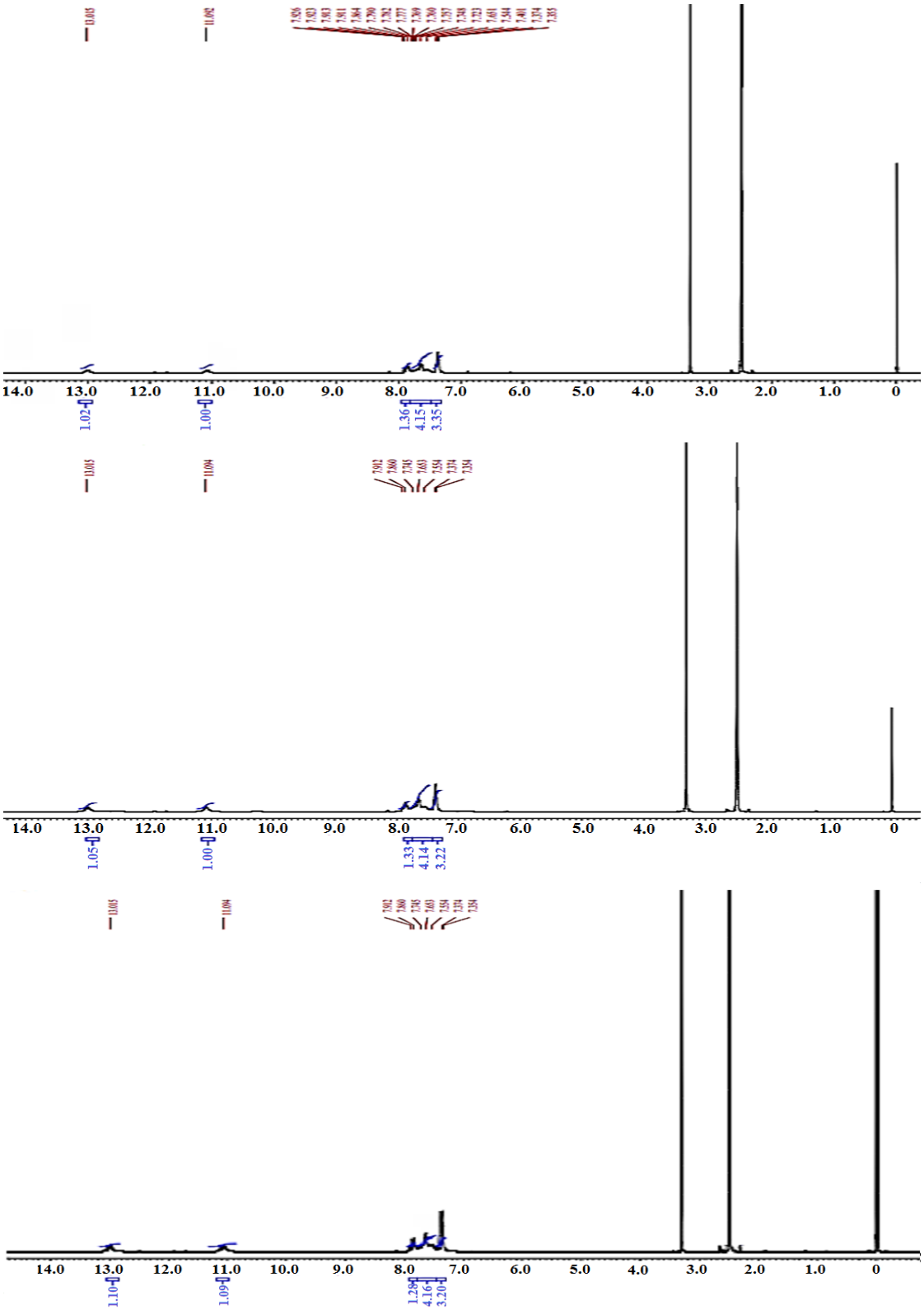

Fig. 5. ^{1}HNMR of AOPDI:Ligand and its VO and Zr acac complexes

Thermogravimetric analysis of L_1 and its complexes

When complexes are heated under regulated experimental conditions, they undergo thermally-induced physical and chemical changes. Thermogravimetric analysis is used to determine how a substance physical properties change with temperature. Basic information on the complexes thermal stability, intermediate residues, final product, and water molecule inclusion is provided. The complexes thermodynamic stability provides information about their lattice and coordinated water. The thermal decomposition of the complexes [VO L_1(acac)] [Zr L_1 $(acac)_3$] given in Table 4 were analysed to confirm the expected structure of the synthesised complex thermal decomposition graph given in Figure 6.

The weight loss caused due to the loss of coordinated water from the complexes was not observed in both the cases. The observed mass loss of 20-21% is attributed to the degradation of OPD moiety which occurred in the temperature range around 301 and 289°C. Decomposition of acac moiety occurs around 304°C. 60% of the weight loss occurs when there is a loss of Alloxan group from coordination complex resulting in the formation of VO_2 as a residue In Zr acac L_1 complexes there is subsequent loss of 3 acac molecules 293 to 310°C with orthophenylene diimine decomposing at an early temperature, suggesting early decomposition of the complexes, whereas degradation of alloxan moiety happens at a very later stage above 325°C giving a residue of ZrO_2 which takes place above 1000°C.

Table 4: TGA data for the L_1 complexes

Sr. No	Complexes	Stage	Temperature range (°C)	%Weight Obs. (cal.)	Species lost	Metallic residue
		1	301.58	73.51 (73.49)	OPD	
1	[L_1VO (acac)]	2	304.34	71.52 (71.49)	acac	VO_2
		3	368.95	39.41 (39.43)	Alloxan	
		1	289.77	82.99 (82.93)	OPD	
		2	293.75	80.64 (80.59)	acac (1)	
2	[L_1Zr $(acac)_3$]	3	295.00	79.91 (79.81)	acac(2)	ZrO_3
		4	300.94	74.70 (74.70)	acac(3)	
		5	325.09	48.76 (48.6)	Alloxan	

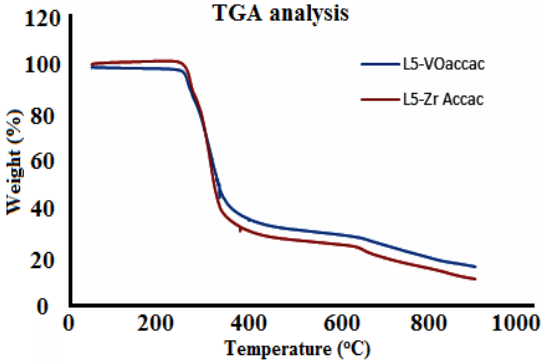

Fig. 6. TGA of L_1:VO and Zr acac complexes

Antibacterial activity

The Table 5 to 7 presents the results of comparing the antibacterial activity of the synthesized metal complexes. The biological effectiveness of the ligand in its free form is associated with the presence of nitrogen in its chemical composition. Metal complexes have moderate activity as a result of the chelation process. Theoretically, the growth of bacteria can be inhibited (bacteriostatic) if electrical charges absorb or displace ionizing disinfectant molecules during the first contact and absorption phase. Metal complexes have greater biological activity than ligands.[15-21]

In order to comprehend the possible modes of action of metal complexes, to evaluate their biological activities structures of ligand and complexes need to be predicted. Microbes can acquire resistance to drugs, there is currently interest in developing novel therapeutic agents with modification in Schiff bases and synthesis of complexes. Metal complexes that contain hetero donor ligands demonstrate significant biological activity while diminishing toxicity. The data in the table suggests L_1 ligand and its complexes specifically did not exhibit greater antibacterial Complexes of L_1 exhibited enhanced activity as compared to ligand for the reason metal exhibited more liphophilicity as compared to ligand. The biological activity of the molecule depends on the presence of hydrogen bonding. According to literature studies, semicarbazones showed enhanced activity like anticonvulsant, antihelmenthetic, antimicrobial properties compared to orthophenyldiimine derived from Alloxan. Zone of inhibition is represented in the Figure 7.

Table 5: Antibacterial Property [L_1-Alloxan-orthophenylene diimine]

Concentration	Microorganism zone of inhibition (in cm)		
	Bacillus cereus	*Escherichia coli*	*Pseudomonas aeruginosa*
100 µg	0.1	-	1.1
200 µg	0.2	-	1.5
300 µg	0.3	-	1.6
400 µg	0.5	-	1.8

Table 6: Antibacterial Property [L_1-Alloxan-orthophenylene diimine-VO (acac)]

Concentration	Microorganism zone of inhibition (in cm)		
	Bacillus cereus	*Escherichia coli*	*Pseudomonas aeruginosa*
100 µg	-	0.3	0.1
200 µg	-	0.5	0.3
300 µg	-	0.7	0.6
400 µg	-	1.2	0.8

Table 7: Antibacterial Property [L_1Alloxan-orthophenylene diimine-Zr $(acac)_3$]

Concentration	Microorganism zone of inhibition (in cm)		
	Bacillus cereus	*Escherichia coli*	*Pseudomonas aeruginosa*
100 µg	-	0.2	-
200 µg	-	0.5	-
300 µg	-	0.7	-
400 µg	-	1.0	-

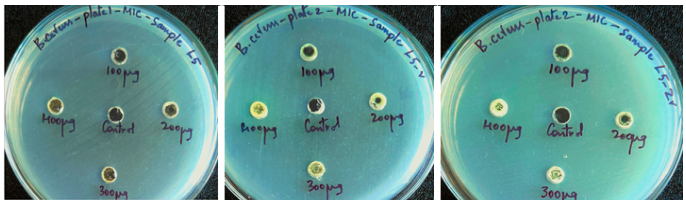

Fig. 7. Zone of Inhibition of Ligand and complexes

Molecular docking studies of Thymidine phosphorylase with L_1 ligand and VO acac complexes

The function of this enzyme are involved in the breakdown of thymidine. It catalyzes the conversion of thymidine to thymine and 2-deoxy-D-ribose-1-phosphate by adding a phosphate group to thymidine. This enzyme is part of the pyrimidine salvage pathway, where cells recycle nucleotides to use them in the synthesis of new DNA.

There are many significance to operate this enzyme, particularly, Thymidine phosphorylase has been studied in the context of cancer. In some tumors, the expression of thymidine phosphorylase is increased. This increased expression has been associated with angiogenesis, the formation of new blood vessels to support tumor growth. As a result, thymidine phosphorylase inhibitors have been explored as potential anticancer agents. Understanding the role of thymidine phosphorylase is important not only for basic cellular processes but also for potential therapeutic interventions in diseases like cancer.

The ligand and its metal complexes are subjected to study the inhibition nature to compare with one another through Vina docking. Docking investigations for ligands L_1 along with VO complexes were carried out. The Vandium complexes, were docked by replacing V parameters by S, P, Ni, Fe, respectively to test their docking performances, in which phosphorus (-6.6 kcal/mol), Sulphur (-7.5 kcal/mol), Ni and Fe docking scores were identified. Among these replacement, Ni and Fe (-8.2 kcal/mol) were producing high scores hence,

we have taken Ni (-8.3 kcal/mol) as replacing atom in place of vanadium[21,22] Vina docking score of L_5, VO acac are displayed in the Table 8.

PDB 1uou enzyme has been taken for Vina docking studies. To inhibit this protein with the synthesised ligands and complexes resulting in inhibition of tumor development is studied with docking scores. The binding affinity of the ligands L_1 and complexes have efficient values such as, -8.9 kcal/mol for L_1. At the same time with metal acac combinations has more score than the L_1. Hence overall Vina docking score for these ligands are having good sign to develop the drugs for tumor. The 2D and 3D interactions are displayed in the following figures and the inhibited amino acids are listed in the table. These amino acids are majorly involved in controlling of tumors.

Table 8: Vina docking scores of L_1 and VO acac complexes

Ligands	Mode	Affinity (kcal/mol)	Distance from best mode	
			Rmsd L.b.	Rmsd U.b.
L_1	1	-8.9	0	0
	2	-8.9	0.2	2.039
	3	-8.7	0.772	1.674
	4	-8.5	0.783	2.628
	5	-8.1	3.509	6.111
L_1 with VO Acac	1	-8.2	0	0
	2	-7.8	2.521	6.44
	3	-6.4	2.876	6.187
	4	-6	2.199	4.276
	5	-5.4	2.025	4.962

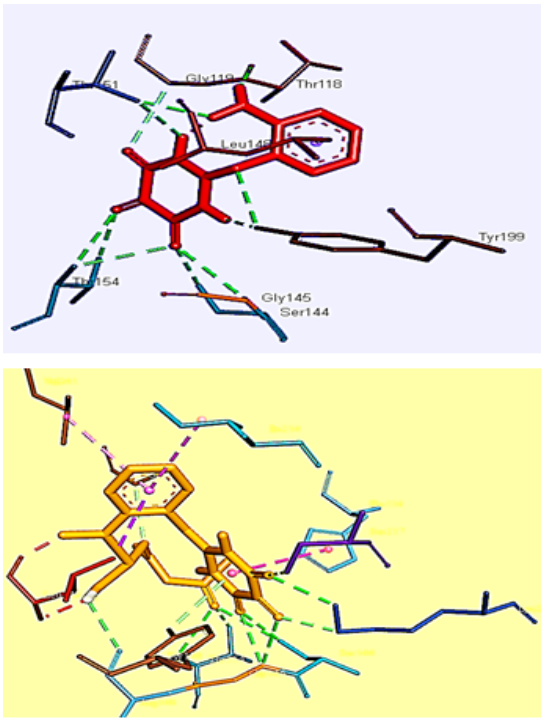

Fig. 8. 3D molecular interaction view of L_1 and VO acac complexes

CONCLUSION

Green method of synthesis of the ligand was found to be effective leading to a sustainable development. Cell line studies of the synthesised ligand and complex can be studied for their antitumour properties. Orthophenylene diamine was condensed with alloxan to form Schiff's Base and formation of metal complexes were indicated with colour change, difference in melting point and molar conductance values.The preferred geometry of the molecule was found to be square pyramidal with bond angle of 118° to 120° for Vanadium complexes. Assumed geometry for Zirconium complexes square antiprismatic.TGA studies confirmed the observed molecular formula suggesting subsequent loss of the species to yield VO_2 and ZrO_3 as a residue. Biological activity involving antibacterial studies revealed less effectiveness in using as a topical agent for dermal regions. The active site amino acids THR118, GLY119, SER144, GLY145, LEU148, THR151, THR154, and TYR199 are more inhibited by the ligand L5 and HIS116, GLY119, SER144,GLY145, ARG146, THR154, TYR199, SER217 and LYS221 are active site amino acids, that are inhibited by the L1-VO metal acac ligand.

ACKNOWLEDGEMENT

PES University Bengaluru,Assyme Bioscience for providing microbial cultures.

Conflicts of Interest

Nil

REFERENCES

1. Beraldo, H.; Gambino, D., Mini reviews in *Medicinal Chemistry*., **2004**, *4*(1), 31-39.
2. Bojarski, J. T.; Mokrosz, J. L.; Barto, H. J.; Paluchowska,M.H., *Advances in Heterocyclic Chemistry*., **1985**, *38*, 229-297.
3. Kumari, Y. P.; Chandra, J. S.; Rao, B. S.; Sunandamma, Y., *Journal of Current Pharmaceutical Research*., **2012**. *10*(1), 28-33.
4. Champion, G. D.; Graham, G. G.; Ziegler, J. B., *Baillière's Clinical Rheumatology*., **1990**, *4*(3), 491-534.
5. Shebaldina, L. S.; Kovalchukova, O. V.; Strashnova, S. B.; Zaitsev, B. E.; Ivanova, T. M., *Russian Journal of Coordination Chemistry*., **2004**, *30*, 38-42.
6. Refat, M. S.; El-Korashy, S. A.; Kumar, D.N; Ahmed, A.S., *Journal of Coordination Chemistry*., **2008**, *61*(12), 1935-1950.
7. Resnik, R. A.; Cecil, H., *Archives of Biochemistry and Biophysics*., **1956**, *61*(1), 179-185.
8. Nuwan De Silva, N. W. S. V.; Lisic, E. C.; Albu, T.V., *Central European Journal of Chemistry*., **2006**, *4*, 646-665.
9. Jayaseelan, P. E.; Akila, M.; Usha Rani; Rajavel, R., *Journal of Saudi Chemical Society*., **2016**, *20*(6), 625-634.
10. Mahapatra, B. B.; Panda, D.; Pujari, S. K., *Transition Metal Chemistry*., **1983**, *8*(2), 119-121.
11. Domazetis, G.; Mackay, M. F.; Magee, R. J.; James, B.D., *Inorganica Chimica Acta*., **1979**, *34*, 47-48.
12. El-Dissouky, A., *Molecular Spectroscopy*., **1987**, *43*(9), 1177-1182.
13. Jayabalakrishnan, C.; Karvembu, R.; Natarajan, K., *Synthesis and reactivity in inorganic and metal-organic chemistry*., **2002**, *32*(6), 1099-1113.
14. Sevinçli, Z.; Duran, G. N.;Özbî L,M.; Karalı,N., *Bioorganic Chemistry*., **2020**, *104*, 104202.
15. Verma, M.; Pandeya, S. N.; Singh, K. N.; Stables, J.P., *Acta Pharmaceutica*., **2004**, *54*(1), 49-56.
16. Singh, G.; Gupta, S.; Esteban, M. A.; Espinosa-Ruíz, C.; González-Silvera, D., *Journal of Molecular Structure*., **2022**, *1255*, 132446.
17. Gandhe, S.; Gautam, M. D., *Asian Journal of Chemistry*., **2004**, *16*(1), 261.
18. Mahmood-ul-Hassan; Chohan, Z. H.; Supuran,C.T., *Synthesis and Reactivity in Inorganic and Metal-Organic Chemistry*., **2002**, *32*(8), 1445-1461.
19. Biswas, A.;Das, L. K.; Drew,M.G.; Diaz, C., Ghosh, A., *Inorganic Chemistry*., **2012**, *51*(19), 10111-10121.
20. Scior,T.; Abdallah, H. H.; Mustafa, S. F. Z.; Guevara-García, J. A.; Rehder, D., *Inorganica chimica acta*., **2021**, *519*, 120287.
21. Nagar, S.; Raizada, S.; Tripathee, N., *Results in Chemistry*., **2023**, 101153.